ARTICLES

Dissociation of Metastable CH_3CO Radical Observed by Subpicosecond Time-Clocked Photofragment Imaging

Takeshi Shibata,[†] Haiyang Li,[‡] Hideki Katayanagi,[‡] and Toshinori Suzuki*[,†,‡]

Graduate University for Advanced Studies, Myodaiji, Okazaki 444-8585, Japan, and Institute for Molecular Science, Myodaiji, Okazaki 444-8585, Japan

Received: August 11, 1997; In Final Form: January 6, 1998

A novel experimental technique to measure the energy-dependent unimolecular dissociation rate $k(E)$ of radical species is presented. Internally-excited CH_3CO radicals were formed by ultraviolet photodissociation of CH_3-COCl, and the subsequent decay of these radicals was detected by subpicosecond time-clocked photofragment imaging. The CH_3CO radicals with different internal energies were dispersed in space by their recoil velocities, and their decay rates were measured for each internal energy. The dissociation rates of CH_3CO radicals determined were an order of magnitude smaller than those calculated by Rice−Ramsperger−Kassel−Marcus theory.

Introduction

Unimolecular reaction of small molecules is governed by detailed dynamics on potential energy surface(s), and it is manifested by characteristic internal state and scattering distributions of the products. In the reaction of large molecules, however, a large phase space is accessed by intramolecular mode coupling, so that it tends to exhibit statistical behavior. In the latter case, the dynamical influence on the internal state and scattering distributions diminishes, and the reaction is characterized by its rate. Experimental investigations of the reaction of large molecules, therefore, are directed to the measurements of reaction rates and the comparison with statistical theories such as Rice−Ramsperger−Kassel−Marcus (RRKM) theory.[1,2]

Reaction rates $k(E)$ have been measured by various energization methods of molecules, such as shock tube, infrared multiphoton absorption, overtone excitation, electronic excitation followed by electronic relaxation, and stimulated emission pumping.[1,2] However, application of these methods to free radicals has been scarce. It is noted that these reactive species have rather low energy barriers for dissociation, so that intramolecular vibrational energy redistribution (IVR) may compete with the dissociation, thereby attracting much attention to the reaction of free radicals. For investigating unimolecular reaction of free radicals, an experimental method that allows efficient excitation of radicals into a range of internal energies and the measurements of the subsequent decay of radicals for each internal energy is necessary. In the present paper, we propose a novel experimental technique that comprises these two features.

The method is schematically shown in Figure 1. The radicals, R, are produced by photodissociation of molecules R−X in a molecular beam. By irradiation of the pump laser pulse, radicals are ejected into space with various internal energies. With a certain pump−probe time delay, the radicals are ionized by multiphoton ionization by a probe laser pulse. When an atom

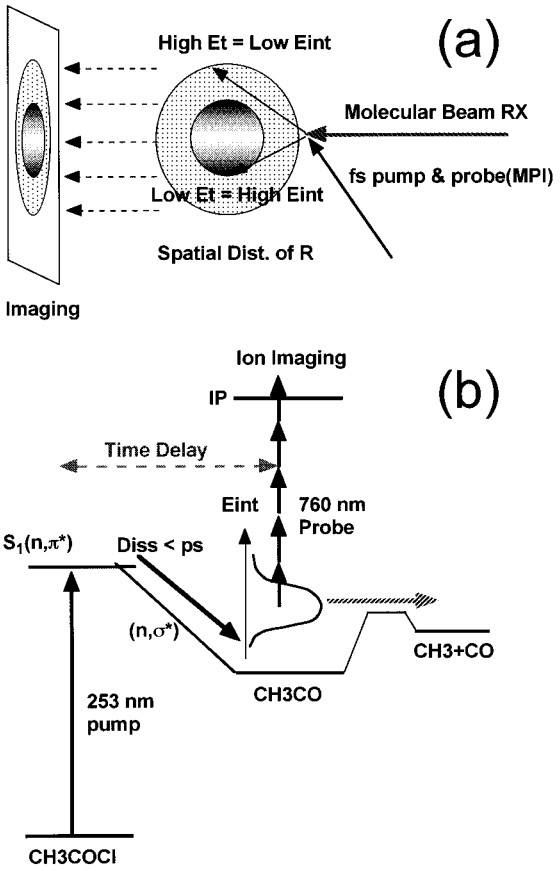

Figure 1. (a) Dispersion of radicals by their translational energy. (b) Energy diagram of photodissociation of acetyl chloride and secondary dissociation of the acetyl radical.

* Author to whom correspondence should be addressed: suzuki@ims.ac.jp.
[†] Graduate University for Advanced Studies.
[‡] Institute for Molecular Science.

S1089-5639(97)02627-3 CCC: $15.00
Published on Web 05/06/1998

X is created in a single quantum state (e.g., the ground state), the translational energy of R will relate with the internal energy of R due to energy and momentum conservation laws. Then, the radicals with small internal energy have large translational energy and are deflected from the molecular beam, while the radicals with larger internal energy have smaller translational energy and remain close to the molecular beam. In this way, the radicals R with different internal energies are dispersed in space and detected by a two-dimensional position sensitive detector.[3−5] If the radical has sufficient internal energy to surmount the barrier for the secondary dissociation R → A + B, it will decompose before being ionized by a probe laser pulse. Disappearance of the radical with a certain translational energy is visualized by two-dimensional ion imaging, so that a series of images taken by varying the pump−probe time delay allows the observation of the decay of energy-dispersed radicals. Time-resolved observation of metastable radicals produced by photodissociation has already been demonstrated by Kim et al.[6−8] The novel feature of our experiment, however, is the dispersion of the radicals R with different internal energy, which is the key to relate the decay rate to the internal energy *E*.

The ultraviolet photodissociation of acetyl chloride has been studied by several workers.[9−15] It is known that the C−Cl bond is immediately dissociated upon photoexcitation to the $^1(n, \pi^*)$ state due to the surface crossing between the $^1(n, \pi^*)$ localized on the C═O bond and $^1(n, \sigma^*)$ localized on the C−Cl bond.[9,14,15] Furthermore, North et al.[10] have obtained an energy barrier value for the secondary dissociation of CH_3CO into CH_3 and CO of 17 ± 1 kcal/mol from the comparison of the translational energy distributions of CH_3CO and Cl fragments in photofragment translational spectroscopy (PTS).[16] Deshmukh et al. have observed CH_3 and CO in 236 nm photodissociation of acetyl chloride, which they assigned to the products of the secondary dissociation of CH_3CO.[11,12] In the present paper, the decay of the metastable CH_3CO radical is observed in real time as a function of its internal energy.

Experimental Section

A supersonic beam, 1 mm in diameter (full width at half-maximum; fwhm), was introduced into a time-of-flight (TOF) mass spectrometer in the direction parallel to the electric field vector.[17,18] A sample gas, <1.25−5% seeded in He, was expanded with a stagnation pressure of 700 Torr relative to the vacuum. The output from an Ar^+ laser-pumped Ti:Sapphire laser was amplified with a regenerative amplifier pumped by a 10 Hz Nd:YAG laser. The time duration and energy of the amplified pulses were 150-200 fs and 6 mJ/pulse (at 765 nm), respectively. The *pump* pulse at 255 nm was generated by sequential doubling and mixing processes in two β-BaB_2O_4 (BBO) crystals. The typical pump laser power used was about 50 μJ/pulse. The fundamental (760 nm) of a 100−800 μJ/pulse was used as a *probe* pulse, and the time delay between the pump and probe pulses was varied with a micrometer-driven optical delay stage. Both pump and probe laser pulses were coaxially aligned with a dichroic mirror and focused ($f = 300$ mm) onto the molecular beam; the probe beam focus was outside of the molecular beam because of chromatic aberration. Typical cross-correlation between the pump and probe pulses was 350 fs (fwhm). Both the pump and probe laser polarization were aligned parallel to the imaging detector to ensure the cylindrical symmetry of ion distributions that is necessary for an inverse Abel transform of the data.

The ions produced were accelerated up to a kinetic energy of 2−5 keV by an electric field and projected onto a micro-channel plate (MCP) backed by a phosphor screen. A high-voltage pulse 1800 V in height and 200−500 ns in duration was applied to the MCP to time-gate CH_3CO^+ ions. Subsequently, a transient image on the screen was captured by a Peltier-cooled CCD camera (512 × 512 pixels) and was accumulated for 18 000−144 000 laser shots. An inverse Abel transform was performed on the 2D data to reconstruct the 3D ion distributions.

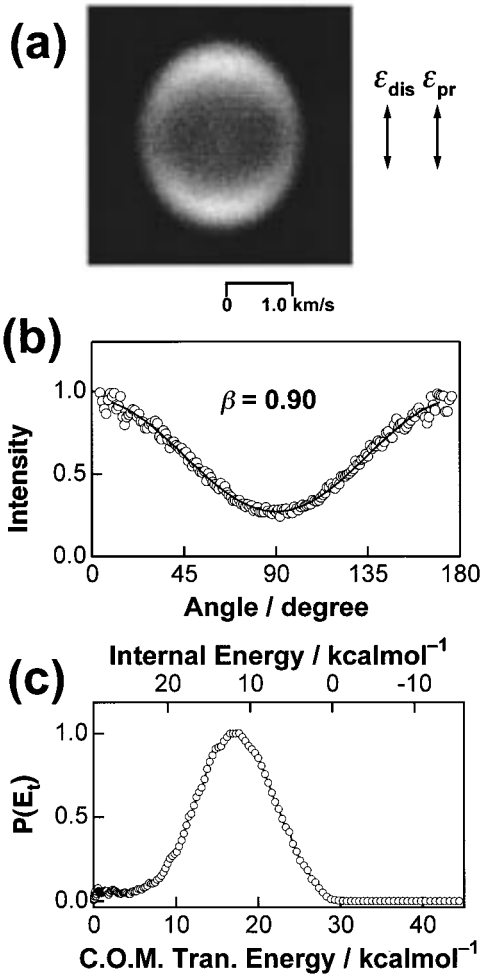

Figure 2. (a) 2D ion image of the CH_3CO radical produced by 255 nm photodissociation of CH_3COCl. The pump−probe time delay is 10 ps, and the pump and probe laser polarization are vertical in the plane. The image was accumulated for 1.4×10^5 laser shots. (b) Angular distribution of the CH_3CO radicals after the dissociation, with center-of-mass translational energy release of 14.6−20.2 kcal/mol. (c) Center-of-mass translational energy release in 255 nm photodissociation of CH_3COCl. The internal energy of CH_3CO produced in the $Cl(^2P_{3/2})$ channels is also indicated.

Results and Discussion

(a) Primary C−Cl Bond Rupture in CH_3COCl. The 2D ion image of CH_3CO produced by 255 nm photodissociation of CH_3COCl is shown in Figure 2a. The pump−probe time delay is 10 ps. This image was obtained by subtracting the one-color background signals due to the pump and probe lasers from the two-color data. It is clearly seen that the CH_3CO radicals are ejected primarily parallel to the pump laser polarization (ϵ_{dis}) which is vertical in the figure. More quantitatively, the angular distribution, $P(\theta)$, was obtained from an inverse Abel transform of the image, as shown in Figure 2b. The distribution was expressed well by the following standard formula:

$$P(\theta) = \sigma/4\pi[1 + \beta P_2(\cos\theta)] \quad (1)$$

where θ is the angle between the electric vector of the pump laser and the recoil velocity, $P_2(x)$ is the second-order Legendre polynomial, and β is an anisotropy parameter. By a least-squares fitting of the formula to the observed data, β was found to be 0.9 ± 0.1, which is in agreement with former reports.[9,13] A high anisotropy indicates that the C−Cl bond rupture occurred faster than molecular rotation of CH_3COCl. For instantaneous dissociation, β is given by $2P_2(\cos\chi)$, where χ is the angle between the transition dipole moment (μ) in the parent molecule and the recoil velocity. From the observed anisotropy parameter, χ is calculated to be $37 \pm 2°$.

The speed distribution, $P(v)$, of CH_3CO was obtained by integrating the angular part of the inverse Abel-transformed data. Then, transformation from the velocity to energy space was performed to obtain center-of-mass translational energy distribution, $P(E_T)$, which is shown in Figure 2c. The translational energy release has a Gaussian shape, in accord with previous studies.[9,10]

(b) Secondary C−C Bond Rupture in CH_3CO. We have measured the ion images of CH_3CO radicals as a function of the pump−probe time delay up to 600 ps, and obtained $P(E_T)$ at each delay time from inverse Abel transforms of the data. Comparing the $P(E_T)$ obtained by independent measurements at the same pump−probe time delay, the experimental uncertainty of $P(E_T)$ has been estimated to be about 10% at each translational energy. The total signal intensity at a certain delay time varied within a factor of 2, due to the change in the alignment of the laser beams, so that the following normalization procedure of $P(E_T)$ was employed. Since the energy barrier for the secondary dissociation of CH_3CO has been estimated to be 17 kcal/mol,[10,19] the $P(E_T)$ corresponding to an internal energy of less than 9 kcal/mol for CH_3CO should be invariant to the pump−probe time delay. Then, the relative intensity, $I(E_1 \le E_T \le E_2,)$ of the particular part of the $P(E_1 \le E_T \le E_2)$, with respect to the $P(E_3 \le E_T \le E_4)$ can be normalized as follows

$$I(E_1 \le E_T \le E_2) = \frac{\int_{E_1}^{E_2} P(E_T)\, dE_T \text{ (metastable part)}}{\int_{E_3}^{E_4} P(E_T)\, dE_T \text{ (stable part)}}$$

In our analysis, we chose $E_3 = 20.2$ and $E_4 = 24.4$ kcal/mol. In Figure 3, the intensities of each translational energy range of interest (=each internal energy due to an energy conservation law) thus obtained are plotted against the delay time.

Note that each decay in Figure 3 exhibits a bimodal feature, either a biexponential or a single exponential with a constant, which is attributed to the two different internal energies of the acetyl radical. Since the counterpart Cl fragment has two accessible spin−orbit states, $^2P_{3/2}$ and $^2P_{1/2}$ separated by 2.5 kcal/mol, each translational energy of CH_3CO actually corresponds to two internal energies of CH_3CO,

$$CH_3COCl \rightarrow CH_3CO + Cl(^2P_{3/2}): \quad E_{int} = E_{avl} - E_{trans}$$

$$\rightarrow CH_3CO + Cl(^2P_{1/2}): \quad E_{int} = E_{avl} - E_{trans} - 2.5 \text{ kcal/mol}$$

The fine structure branching [Cl*]/([Cl] + [Cl*]) in 236 nm photodissociation of acetyl chloride has been reported to be 0.4 ± 0.02 by Deshmukh et al.,[11] so that formation of Cl* cannot be neglected. Distribution of the internal energy of CH_3CO due to the frequency width of the pump laser pulse ($\Delta h\nu \approx 0.5$ kcal/mol) was negligible.

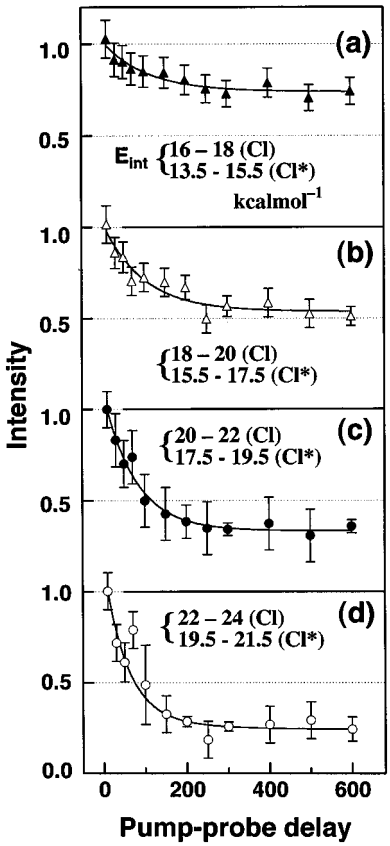

Figure 3. Signal intensity of CH_3CO with different internal energy observed by varying pump−probe time delay. The error bars shown correspond to 10% of each value. Note that each translational energy corresponds to two internal energies of the acetyl radical due to the two spin−orbit states of a Cl atom: (a) 17 ± 1 and 14.5 ± 1; (b) 19 ± 1 and 16.5 ± 1, 21 ± 1 and 18.5 ± 1; (c) 23 ± 1 and 20.5 ± 1 kcal/mol.

Though there is a paucity of data on the excited electronic state of the acetyl radical, it has been suggested that the first excited doublet state is located at about 30 kcal/mol higher than the ground state,[20,21] which is not accessible in the present experiment. Furthermore, from the electronic configuration, the dissociation leading to the excited state of CH_3CO seems unlikely. Thus, the formation of the metastable excited electronic state of the acetyl radical can be ruled out.

In Figure 3, it is clearly seen that the radicals with higher internal energies decay faster. More quantitatively, the decay rates at each internal energy have been estimated by least-squares fitting of a single-exponential or double-exponential decay to each plot, as shown in Figure 4. For comparison, RRKM calculations were performed to estimate the unimolecular dissociation rate of the acetyl radical. Fundamental vibrational frequencies and the vibrational frequencies at the transition state reported by Deshmukh et al.[12] (MP2/cc-pVTZ) were employed. As seen in Figure 5, the decay rates observed for each internal energy were an order of magnitude smaller than those calculated by RRKM theory.

The dissociation rates shown in Figure 4 were calculated by assuming harmonic oscillators for all vibrational modes; however, the agreement with the experimental data is not much improved by anharmonic correction of the vibrations. Anharmonic correction of stretching vibrations reduces the RRKM rate calculated; however, this correction is estimated to be within

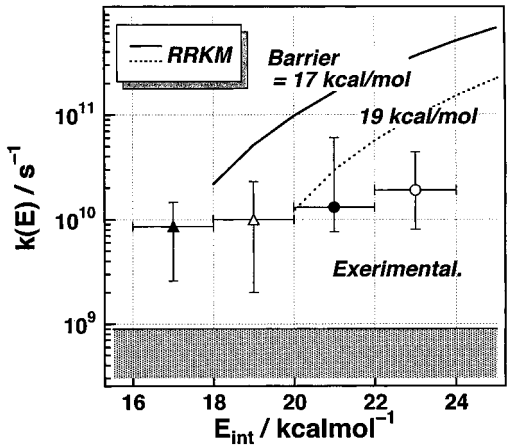

Figure 4. Dissociation rate obtained from subpicosecond time-clocked imaging by single-exponential fitting. Same symbols are used for the decay rate plotted in this figure and the decay curve presented in Figure 3, from which the rate has been determined. Variation of signal intensity of 10% and a limited observation time up to 600 ps do not allow us to determine the decay rate in the shaded area. The solid line shows the RRKM rate calculated for a barrier height of 17 kcal/mol and the broken line for 19 kcal/mol, where no rotational excitation is assumed.

a factor of 2, and cannot account for the discrepancy between calculation and experimental result. When CH_3 torsion is approximated by a free rotor, the RRKM rate increases.[22]

The agreement between the observed rate and an RRKM calculation can be improved if the barrier is higher than 17 kcal/mol. Watkins and Word have suggested 17 kcal/mol by extensive kinetics mesurements,[19] and North et al. suggested 17 ± 1 kcal/mol by PTS.[10] On the other hand, recent ab initio calculations at the MP2/cc-pVTZ level have provided a larger barrier height of 18.7 kcal/mol.[12] However, more accurate ab initio calculations (6-311++G/MP4SDTQ) predict a lower barrier height of 16.3 kcal/mol (with zero-point energy correction).[23] Thus, the barrier height is best estimated to be 17 ± 1 kcal/mol and not higher. In fact, acetyl radical with $E_{int} \sim 17$ kcal/mol seems decaying, indicating that the real barrier could be even lower than 17 kcal/mol. Thus, the discrepancy is presumably attributed to dynamical effects.

One possible dynamical effect to be considered is restricted IVR in the acetyl radical. If the initial internal energy is partitioned to vibrational modes which are poorly coupled with C−C stretching, the apparent reaction rate will be smaller than RRKM theory. Another effect could be rotational metastability of the acetyl radical. Since acetyl chloride becomes pyramidal in the ^{1}(n, π^*) state, it is also pyramidal at the surface crossing point between the ^{1}(n, π^*) and ^{1}(n, σ^*) states.[14,15] Therefore, the subsequent C−Cl repulsion is expected to excite molecular rotation of CH_3CO around its *a*-axis. The *a*-axis rotation is not expected to be strongly coupled with the C−C dissociation coordinate, thus leading to a smaller dissociation rate than RRKM theory; for instance, if *a*-axis rotation is completely inactive in reaction, rotational excitation reduces the available energy for the reaction. *K*-scrambling due to Coriolis coupling will diminish the reduction of reaction rate, since it allows the system to sample low *K* states with a lower effective barrier for the reaction due to centrifugal force. If *K*-scrambling is restricted, it will become rotationally metastable.

As for the rotational metastability, accurate estimation of the rotational excitation of acetyl radical cannot be made unfortunately due to the lack of information on the potential energy surface of acetyl chloride. A soft impulsive model (the model considering the conservation of linear momentum between C and Cl atoms) with the geometry at the crossing point of ^{1}(n, π^*) and ^{1}(n, σ^*) calculated by the ab initio method[15] predicts that the acetyl radical is excited around the *a*-axis with an energy of 14 kcal/mol, which is considered to be an overestimation. Since the acetyl radical is relaxed gradually to the planar structure on the ^{1}(n, σ^*) surface, C−Cl stretching is strongly coupled with C−Cl bending. This leads to smaller rotational excitation of the acetyl radical. It is noted that an impulsive model is only applicable to the system where anisotropy of the PES is small.[24]

Kim et al. have performed femtosecond pump−probe mass spectrometry on photodissociation of acetone, diethyl ketone, and methyl ethyl ketone.[6−8] These molecules were excited by two-photon absorption of 307 nm light, which induced the primary C−C bond cleavage within 100 fs. It was found that the metastable CH_3CO and C_2H_5CO radicals thus produced have lifetimes of 550−900 fs which are about an order of magnitude longer than those predicted by RRKM theory.[6−8] Due to the difference in the primary dissociation mechanism and in energetics between the experiment by Kim et al.[6−8] and ours, internal excitation of CH_3CO is quite different. Nonetheless, both experiments point to the discrepancy between the experimental result and statistical calculations in the dissociation of the CH_3CO radical.

Conclusion

Subpicosecond time-clocked photofragment imaging was employed to measure the energy-dependent dissociation rate $k(E)$ of radical species. The CH_3CO radicals were formed by ultraviolet photodissociation of CH_3COCl, and the subsequent decay of these radicals was observed. The decay rates observed for each internal energy were an order of magnitude smaller than those calculated by RRKM theory. It is likely that IVR and/or vibration-rotation energy exchange prior to C−C bond rupture is restricted. The present study demonstrates the potential of time-resolved photofragment imaging for the study of unimolecular reaction of free radical species.

Acknowledgment. We thank Professor Mutsumi Aoyagi for helpful discussions and ab initio calculations. We also thank Professor Ming-Chang Lin for providing us with the RRKM reaction rate and Dr. Imitaz Ahmed for careful reading of the manuscript. This work was partially supported by the Ministry of Education, Science, Sports and Culture (08559014 and 09440208) and the New Energy and Industrial Technology Development Organization.

References and Notes

(1) Holbrook, K. A.; Pilling, M. J.; Robertson, S. H. *Unimolecular Reactions*; 2nd ed.; John-Wiley and Sons: New York, 1996.

(2) Baer, T.; Hase, W. L. *Unimolecular Reaction Dynamics; Theory and Experiments*; Oxford Univ. Press: Oxford, 1996.

(3) Chandler, D. W.; Houston, P. L. *J. Chem. Phys.* **1987**, *87*, 1445.

(4) Heck, A. J. R.; Chandler, D. W. *Annu. Rev. Phys. Chem.* **1995**, *46*, 335.

(5) Whitaker, B. J. In *Research in Chemical Kinetics I*; Compton, R. G., Hancock, G., Eds.; Elsevier: New York, 1993.

(6) Kim, S. K.; Pedersen, S.; Zewail, A. H. *J. Chem. Phys.* **1995**, *103*, 477.

(7) Kim, S. K.; Zewail, A. H. *Chem. Phys. Lett.* **1996**, *250*, 279.

(8) Kim, S. K.; Guo J.; Baskin, J. S.; Zewail, A. H. *J. Phys. Chem.* **1996**, *100*, 9202.

(9) Person, M. D.; Kash, P. W.; Butler, L. J. *J. Chem. Phys.* **1992**, *97*, 355.

(10) North, S. W.; Blank, D. A.; Lee, Y. T. *Chem. Phys. Lett.* **1994**, *224*, 38.

(11) Deshmukh, S.; Hess, W. P. *J. Chem. Phys.* **1994**, *100*, 6429.

(12) Deshmukh, S.; Myers, J. D.; Xantheas, S. S.; Hess, W. P. *J. Phys. Chem.* **1994**, *98*, 12535.
(13) Shibata, T.; Suzuki, T. *Chem. Phys. Lett.* **1996**, *262*, 115.
(14) Martin, X.; Moreno, M.; Lluch, J. M. *J. Phys. Chem.* **1993**, *97*, 12186.
(15) Sumathi, R.; Chandra, A. K. *J. Chem. Phys.* **1993**, *99*, 6531.
(16) Busch, G. E.; Wilson, K. R. *J. Chem. Phys.* **1972**, *56*, 3626.
(17) Suzuki, T.; Tonokura, K.; Bontuyan, L. S.; Hashimoto, N. *J. Phys. Chem.* **1994**, *98*, 13447.
(18) Tonokura, K.; Daniels, L. B.; Suzuki, T.; Yamashita, K. *J. Phys. Chem. A.* **1997**, *101*, 7754.
(19) Watkins, K. W.; Word, W. W. *Int J. Chem. Kinet.* **1974**, *6*, 855.
(20) Nimlos, M. R.; Soderquist, J. A.; Ellison, G. B. *J. Am. Chem. Soc.* **1989**, *111*, 7675.
(21) Jacox, M. E. *J. Phys Chem. Ref. Data.* **1988**, *17*, 269.
(22) Kristian, S.; Lin, M. C. Private communication.
(23) Aoyagi, M. Private communication.
(24) Schinke, R. *Photodissociation Dynamics*; Cambridge Univ. Press: Cambridge, 1993.